

# Secondary Leaflet Tethering in Patients with degenerative mitral regurgitation and its Association with the Severity of Mitral Regurgitation

Zhenyi Ge<sup>1</sup>, Chunqiang Hu<sup>1</sup>, Fangyan Tian<sup>1</sup>, Yingjie Zhao<sup>1</sup>, Yongshi Wang<sup>1</sup>, Dehong Kong<sup>1</sup>, Wei Li<sup>1</sup>, Yashu Xie<sup>2</sup>, Zhengdan Ge<sup>1</sup>, zibire fulati<sup>1</sup>, Yufei Cheng<sup>1</sup>, Yao Guo<sup>1</sup>, Yingying Jiang<sup>1</sup>, Cuizhen Pan<sup>1</sup>, and Xianhong Shu<sup>1</sup>

<sup>1</sup>Zhongshan Hospital Fudan University

<sup>2</sup>ChengDu Healthcare Security Administration

April 28, 2023

## Abstract

**Background** The purpose of the study was to determine the association between vena contracta area (VCA) and secondary leaflet tethering among mitral valve prolapse (MVP) patients, and thus to further identify and characterize an MVP with pathological leaflet tethering (MVPt+) phenotype. **Methods** We prospectively evaluated 94 consecutive MVP patients with significant mitral regurgitation (MR) and 20 healthy controls. MVPt+ group was defined as tenting volume index (TVi) > 0.7 ml/m<sup>2</sup>. The three-dimensional (3D) geometry of mitral valve apparatus and VCA was measured with dedicated quantification software. **Results** Of the 94 patients with MVP and significant MR, 31 patients showed a TVi > 0.7 ml/m<sup>2</sup> and entered the MVP with leaflet tethering (MVPt+) group. In stepwise multivariate analysis, only prolapse volume index and TVi was independently associated with 3D VCA. Apart from marked left ventricular and annular enlargement, MVPt+ group presented significantly higher frequency of leaflet flail, greater VCA, elevated plasma levels of NT-proBNP and sPAP. ROC curve revealed that occurrence of leaflet tethering is associated with a VCA [?]0.55 cm<sup>2</sup> in MVP patients. **Conclusions** Secondary leaflet tethering is a significant mechanism behind severe degenerative mitral regurgitation, resulting an MVPt+ phenotype featuring more advanced morphological and hemodynamical characteristics .

## Secondary Leaflet Tethering in Patients with degenerative mitral regurgitation and its Association with the Severity of Mitral Regurgitation

Zhenyi Ge<sup>1,2</sup>, MD, Chunqiang Hu<sup>1,2</sup>, MD, Fangyan Tian<sup>1,2</sup>, MD, Yingjie Zhao<sup>1,2</sup>, MD, Yongshi Wang<sup>1</sup>, MD, Dehong Kong<sup>1</sup>, MD, Wei Li<sup>1</sup>, MD, Yashu Xie<sup>3</sup>, MD, Zhengdan Ge<sup>1,2</sup>, MD, Zibire Fulati<sup>1</sup>, MD, Yufei Cheng<sup>1</sup>, MD, Yao Guo<sup>1</sup>, MD, Yingying Jiang<sup>1</sup>, MD, Cuizhen Pan<sup>1,2</sup>, MD, Xianhong Shu<sup>1,2</sup>, MD, PhD

<sup>1</sup>Department of Echocardiography, Shanghai Institute of Cardiovascular disease, Zhongshan Hospital, Fudan University, Shanghai, China

<sup>2</sup>Shanghai Institute of Medical Imaging, Fudan University, Shanghai, China

<sup>3</sup>ChengDu Healthcare Security Administration, Sichuan, China

Drs. Zhenyi Ge, Chunqiang Hu and Fangyan Tian are co-first authors.

Drs. Cuizhen Pan and Xianhong Shu contributed equally to this work and should be considered co-corresponding authors.

Corresponding to: Cuizhen Pan or Xianhong Shu

Address: Department of Echocardiography, Zhongshan Hospital, Fudan University, No.1609 Xietu Road, Xuhui District, Shanghai, China.

E-mail: pan.cuizhen@zs-hospital.sh.cn or shu.xianhong@zs-hospital.sh.cn

## Abstract

**Background** The purpose of the study was to determine the association between vena contracta area (VCA) and secondary leaflet tethering among mitral valve prolapse (MVP) patients, and thus to further identify and characterize an MVP with pathological leaflet tethering (MVPt+) phenotype.

**Methods** We prospectively evaluated 94 consecutive MVP patients with significant mitral regurgitation (MR) and 20 healthy controls. MVPt+ group was defined as tenting volume index (TVi)  $> 0.7$  ml/m<sup>2</sup>. The three-dimensional (3D) geometry of mitral valve apparatus and VCA was measured with dedicated quantification software.

**Results** Of the 94 patients with MVP and significant MR, 31 patients showed a TVi  $> 0.7$  ml/m<sup>2</sup> and entered the MVP with leaflet tethering (MVPt+) group. In stepwise multivariate analysis, only prolapse volume index and TVi was independently associated with 3D VCA. Apart from marked left ventricular and annular enlargement, MVPt+ group presented significantly higher frequency of leaflet flail, greater VCA, elevated plasma levels of NT-proBNP and sPAP. ROC curve revealed that occurrence of leaflet tethering is associated with a VCA  $[?]0.55$  cm<sup>2</sup> in MVP patients.

## Conclusions

Secondary leaflet tethering is a significant mechanism behind severe degenerative mitral regurgitation, resulting an MVPt+ phenotype featuring more advanced morphological and hemodynamical characteristics.

**Keywords:** 3D transesophageal echocardiography; mitral valve prolapse; degenerative mitral regurgitation; mitral valve geometry

## Introduction

Mitral valve (MV) prolapse (MVP), as the most common finding in degenerative mitral regurgitation, is defined by superior displacement during systole of the free edge of leaflet beyond the annular level, resulting in coaptation failure and mitral regurgitation (MR).<sup>[1, 2]</sup> Conventional two-dimensional (2D) echocardiographic studies showed it frequently accompanied with varied degrees of annular dilation, leaflet redundancy, and chordal dysfunction.<sup>[3, 4]</sup>

MVP tends to progress over time with increase in volume overload. Moreover, left ventricular remodelling can begin with even mild MR as a continuous adaptive process to volume overload and progresses that paralleled to MR severity. <sup>[5-7]</sup>

Three-dimensional (3D) transesophageal echocardiography (TEE) could provide excellent images of MV apparatus and accurate measurements of the mitral complex and has increase our understanding of DMR disease. Recent study using 3D TEE has revealed that left ventricular remodelling in MVP patients can exacerbate mal-coaptation through apical tethering of non-prolapsed leaflet segments, constituting a vicious MR-tethering cycle.<sup>[8]</sup> Subsequently, leaflet tethering in MVP patients has been reported to be associated with residual MR after surgical repair and transcatheter edge-to-edge repair.<sup>[9-11]</sup> However, it remains unclear about how severe the MR is when the MR-tethering cycle is triggered. One of the possible reasons may be lack of specific criteria for differentiating normal from pathological leaflet tethering in MVP patients. Indeed, limitations existed with the small population and narrow spectrum of MR severity in the previous study.<sup>[8]</sup>

The goals of this study were using 3D TEE determine the association between vena contracta area (VCA) and secondary leaflet tethering among MVP patients, and thus to further identify and characterize an MVP with pathological leaflet tethering (MVPt+) phenotype.

## Methods

### Patient population

From July 2018 to December 2020, a total of 117 consecutive patients with degenerative mitral valve disease and significant MR (grade 2+) in a prospective multicenter study underwent transthoracic and transesophageal echocardiographic assessment and were included in the study.

Twenty-three were excluded for the following reasons: (1) 10 were excluded owing to inadequate echocardiographic image quality for MVN or 3D VCA analysis; (2) 7 were excluded because of with mixed atrial functional mitral regurgitation or presence of mitral annular disjunction; (3) 4 were excluded because of significant concomitant aortic valve disease; (4) 2 was excluded due to having abnormal segmental wall motion. Twenty subjects (ages  $67 \pm 8.5$ ) undergoing clinically indicated TTE and TEE who have no MR with normal left ventricular (LV) function and mitral apparatus were also examined as controls. The protocol of this study was approved by the institutional review board of Zhongshan Hospital and was conducted in accordance with the Declaration of Helsinki. Written informed consent was obtained at the time of consent for the clinical TEE procedure in all of the patients.

### MVN analysis

The Mitral Valve Navigation (MVN) analysis was performed as previously described.<sup>[11]</sup> Imaging data sets were analyzed by the core laboratory echocardiographer using Philips Mitral Valve Navigation software (Qlab version 13; Philips Medical Systems). Images with the highest volume rate ([?] 10 Hz) and best image quality were selected for analysis. The MVN software provides semiautomated 3D modeling and quantification of the mitral annulus and apparatus (Figure 1). Measurements were performed by two core laboratory echocardiographers, which were blinded to the result of 3D VCA. The mean of three measurements of each parameter was calculated and reported as final value.

The end-systolic frame was identified as the last systolic frame just before aortic valve closure and selected to perform MVN analysis. For the definition of annulus geometry, we assessed anterior–posterior (AP) diameters, lateral/medial (ALPM) diameters, annulus height, annulus area and circumference, and the MV annular ellipticity (defined as ALPM/AP diameter). The ratio of annular height to commissural width (AHCWR) was computed as a surrogate of annular saddle-shaped flattening.<sup>[7]</sup> Severity of prolapse or leaflet tethering was quantified using prolapse height/volume or tenting height /volume, respectively. Two-dimensional and 3D echocardiographic parameters were index to body surface area (BSA) as appropriate, such as AP diameter index (APi).

Secondary leaflet tethering (MVPt+ group) was defined as tenting volume index (TVi)  $> 0.7 \text{ ml/m}^2$ , based on the scatterplot of TVi of our MVP patients and normal value for healthy subjects (Figure 2A). Note that there are no references regarding the threshold of normal values of tenting volume index (TVi) in the literature.<sup>[12, 13]</sup>

### 3D VCA analysis

Three-dimensional color Doppler dataset was acquired to perform off-line analysis of 3D vena contracta area (VCA). Care was taken to include the entire proximal convergence region in the data set with the highest volume rate. The Nyquist limit was controlled within 50–60 cm/s for optimal visualization of the MR jet. Using the commercial software 3DQ (Cardiac 3D Quantification; Philips Medical Systems), the two-orthogonal long-axis planes were aligned parallel with the direction of the proximal MR jet. The transverse plane was then scanned proximally to distally in order to identify the narrowest portion of the jet immediately distal to the regurgitant orifice. The resultant short-axis image of the VC was traced to obtain the 3D VCA.<sup>[14]</sup>

### Statistical analysis

Data are expressed as mean  $\pm$  SD, median (interquartile range), or number of patients (percentages) as appropriate. Normality of all continuous data was confirmed with the Kolmogorov-Smirnov test. Group

comparisons for baseline characteristics, 2D and 3D echocardiographic parameters used analysis of variance (ANOVA), Kruskal-Wallis test, chi-square test, or Fisher exact test as appropriate. Univariate and multivariate linear regression analyses were performed to identify MV 3D geometric variables associated with 3D VCA. Degenerative variables of mitral valve morphology previously shown to be associated with MR in MVP were tested. Variables with P values  $[?] 0.07$  on univariate analysis were tested in the multivariate linear regression with stepwise method. The association between the TVi and other morphological variables was investigated with Pearson correlation analysis. A receiver operating characteristic (ROC) curve was drawn to identify the cutoff value of 3D VCA for MVPt+.

## Results

### Determinants of 3D Vena Contracta Area

All MVP patients presented significant and holosystolic MR. Morphological determinants of 3D VCA are summarized in Table 1. In univariate analysis, factors significantly associated with 3D VCA included annular area index (AAi), prolapse volume index (PVi), TVi and PV + TV and AHCWR. In stepwise multivariate analysis, only PVi and TVi was independently associated with 3D VCA.

### Clinical and 2-Dimensional Echocardiographic Characteristics

Clinical and two-Dimensional Echocardiographic Characteristics are listed in Table 2. Of the 94 patients with MVP and significant MR, 31 patients showed a TVi  $> 0.7 \text{ ml/m}^2$  and entered the MVP with tethering (MVPt+) group, while the rest MVP patients entered the MVP without tethering (MVPt-) group.

There were no differences in age, gender, body surface area and Society for Thoracic Surgeons (STS) risk score ( $P = \text{NS}$  for all). The frequency of NYHA functional class III/IV was slightly higher in MVPt+ group, but this difference did not reach statistical significance ( $P > 0.05$ ). Levels of NT-proBNP and sPAP was markedly elevated in MVPt+ patients.

In addition, MVPt+ group also had larger 3D VCA, LV volume index, max and mean MV gradient ( $P < 0.01$  for all), but similar max VCW compared with MVPt- group. The frequency of leaflet flail in the MVPt+ group was significantly higher than in the MVPt- group (94% vs 73%,  $P = 0.034$ ). Flail/coaptation gap was larger in MVPt+ group and prolapse width was comparable between the two groups.

### Quantitative 3D analysis of MV Characteristics

The geometry of mitral complex in healthy controls, MVPt- and MVPt+ patients are summarized in Table 3. Expectedly, MVPt+ group had a significantly higher tenting volume index (TVi), while MVPt- group had a similar TVi to normal controls.

AML TVi and AML angle was comparable in normal controls and MVPt- group, but MVPt+ group had a significantly larger AML angle. Interestingly, PML TVi and PML Angle was lowest in MVPt- group, intermediate in normal controls, and highest in MVPt+ group. (Figure 2B). Annular dimensions, including ALPM diameter, AP diameter and AAi and annular circumference index, were significantly different among the groups, being lowest in normal controls, intermediate in MVPt- group, and highest in MVPt+ group (Figure 2C).

MVP patients (MVPt- and MVPt+ group) had a larger prolapse height index (PHi) and PVi compared with normal group. Notably, MVPt- patients had significantly larger PHi and PVi compared with MVPt+ patients (Figure 2D).

MVPt+ group was not associated with a lower AWCHR as AWCHR is comparable among three groups (Figure 1E).

### Correlations between tenting volume index and other morphological variables

A mild relationship was observed between TVi and 3D VCA ( $r = 0.56$ ,  $P < 0.001$ ) (Figure 3B). The correlations between TVi and PVi were negative and significant ( $r = -0.319$ ,  $p = 0.0017$ ), while AAi ( $r = 0.459$ ,  $p <$

0.001) correlated positively and significantly with TVi.

NT-proBNP also mildly correlated with TVi ( $r = 0.387$ ,  $p < 0.001$ ) (Figure 3A), whereas no significant association was found between NT-proBNP and PVi ( $P = 0.648$ ).

ROC analysis showed that a 3D VCA  $[?]0.55 \text{ cm}^2$  was the optimal cutoff point for predicting the occurrence of MVPt+ (area under curve 0.82; 95% CI, 0.74-0.91;  $P < 0.001$ ) with a sensitivity of 98% and specificity of 57% (Figure 3C).

## Discussion

The present study conducted provides new information on the 3D MV geometry focusing on leaflet tethering and its association with 3D VCA, with a large population of MVP patients.

The principal finding of the present study is that, secondary leaflet tethering is a significant mechanism behind severe degenerative mitral regurgitation, resulting an MVPt+ phenotype featuring more advanced morphological and hemodynamical characteristics.

In detail, (1) we corroborated that TVi and PVi, rather than annular dimension, were the major independent determinants of 3D VCA in MVP patients with significant MR (2) we carefully defined a cutoff value to characterize the occurrence of pathological leaflet tethering in MVP patients (MVPt+ group) (3) apart from marked LV and annular enlargement, MVPt+ group presented significantly greater 3D VCA, elevated plasma levels of NT-proBNP and sPAP (4) Occurrence of leaflet tethering is associated with a 3D VCA  $[?] 0.55 \text{ cm}^2$  in MVP patients and it could be a specific marker for severe MR (Figure 4). Our findings may bring new insights into risk stratification and surgical decision making to MVP patients.

### Determinants of degenerative mitral regurgitation severity

MR severity for MVP patients varies from trivial to severe according to the failure of coaptation driven by leaflet prolapse or chordal elongation and annular enlargement. <sup>[3, 15]</sup> It tends to progress over time with increase in volume overload (regurgitant volume) due to increase in regurgitant orifice. Progression of MVP is determined by progression of lesions, particular a new flail leaflet, or mitral annulus size. <sup>[4, 16]</sup> In addition, left ventricular enlargement is a continuous adaptive process that begins with even mild MR and progresses paralleled to MR severity.<sup>[5, 17, 18]</sup>

Otani et al. first reported AML tenting volume was proportional to papillary muscle displacement attributed to both annular and LV dilatation, suggesting that degenerative MV prolapse causes secondary LV dilatation and mitral leaflet tethering, especially in non-prolapsed leaflets. <sup>[8]</sup> More recently, Morningstar<sup>[19]</sup> et al demonstrated that mechanical changes induced by a prolapsing valve can engender fibrosis within the inferobasal wall and attached PM that are physically and mechanically linked to the prolapsing leaflets. These changes may also contribute to leaflet tethering in MVP.<sup>[20]</sup>

Previous studies have revealed that prolapse and tenting volume, annular dimension and AHCWR correlated with MR severity in MVP patients.<sup>[4, 7]</sup> We tested these factors in the multivariate model and found that only PVi and TVi was associated with 3D VCA, independent of annular dimension. Indeed, in functional MR (FMR), isolated annular dilation does not usually cause important MR without leaflet tethering caused by LV dilation and dysfunction.<sup>[8, 21]</sup> Although annular dilation is not the most significant determinant of 3D VCA, it contributed to the severity of leaflet tethering. <sup>[8]</sup>

Despite further annular dilatation, our MVPt+ group showed similar AHCWR with normal controls and MVPt- patients. Flattening of annular saddle shape is commonly seen in MAD patients as an intrinsic annular abnormality, which is our exclusion criteria for the current study. Flattening of annular saddle shape also recently has been demonstrated to be correlated with reduction of LV longitudinal contraction (GLS) in atrial FMR. <sup>[22, 23]</sup> Indeed, annular saddle shape is more preserved in FED phenotype<sup>[6]</sup>, which represents the majority of our patients.

It had been widely accepted that leaflet tethering plays a fundamental role in the pathogenesis of FMR<sup>[12, 21]</sup>,

whereas leaflet tethering in MVP patients was not commonly recognized until Otani et al. Although Otani et al.<sup>[12]</sup> firstly elaborated the mechanism, limitations existed with the small population and narrow spectrum of MR severity in the previous study. Furthermore, data on clinical and echocardiographic characteristics MVPt+ patients are sparse. One of the reasons may be attributed to lack of specific criteria for differentiating normal from pathological leaflet tethering in MVP patients.

Under normal physiological circumstances, longitudinal LV fiber contraction translates the posterior annulus apically during the systole as to fold the annulus into a saddle shape. Accordingly, the anterior annulus has to tilt posteriorly, thus made the anterior leaflet tethered at the aortic root.<sup>[24, 25]</sup> The value of TVi in healthy controls and MVPt- group represents the above conformational changes of the anterior leaflet.

Our study also suggested that within MVP patients both AML and PML could occur secondary leaflet tethering, as quantitated by TVi and leaflet angle. Reduction of PML TVi and leaflet angle in MVPt- patients was probably a morphological consequence of PML prolapse.

### **Characteristics of MVP patients with pathological leaflet tethering**

In patients categorized by MVN analysis as MVPt+, we demonstrated more severe clinical and echocardiographic characteristics. Apart from marked LV and annular enlargement, MVPt+ group presented significantly greater MR severity, elevated plasma levels of NT-proBNP and sPAP. All these factors have been shown to be correlated with adverse outcome in MVP patients.<sup>[26] [27]</sup>

Patients in our study with 3D VCA < 0.55 cm<sup>2</sup> had a very low likelihood of being categorized as MVPt+ with a calculated negative predictive value of 98%. Herein, occurrence of leaflet tethering is a specific marker for severe MR (3D VCA [?]0.55 cm<sup>2</sup>) within MVP patients.

### **Clinical Implications**

The concept that secondary leaflet tethering is a significant mechanism behind severe degenerative mitral regurgitation has several clinical consequences. First of all, our study corroborated a pathophysiologic rationale for early surgical repair. Secondly, emphasis may be given to leaflet tethering quantification for MVP patients during the routine echocardiographic evaluation as to assist in MR severity grading and risk stratification. Finally, MV repair for PML prolapse is an established procedure<sup>[1]</sup>, whereas studies regarding MV repair for MVPt+ patients are sparse. Otani et al. demonstrated that MV repair for MVPt+ patients alleviate leaflet tethering and even restore it to normal range, reflecting a favorable surgical result. <sup>[8]</sup> Sakaguchi et al. reported leaflet tethering in MVP could pose challenge to surgical repair as a risk factor for MR occurrence.<sup>[9]</sup> As the above studies were limited with small sample size, whether secondary leaflet tethering in MVP impacts the result of MV repair or whether it could be a complementary therapeutic target should be further investigated in a larger patient group.

### **Limitations**

First of all, this is a cross-sectional study without longitudinal follow-up. To fully understand the prognostic role of leaflet tethering in patients with MVP, follow-up studies in valvular determinants for the adverse outcome should be carried out. In addition, the study sample, featuring with a majority of FED etiology, presence of symptoms, is derived from patients enrolled in a multicenter registry to assess suitability for transcatheter edge-to-edge repair. Thus, selection bias cannot be ruled out in the present study. The majority presented symptomatic severe mitral regurgitation requiring MV surgery. Finally, as is previously described, the last-systolic frame was chosen to analyze 3D morphological parameters as it typically presented the largest prolapse magnitude and the minimal tenting magnitude.

### **Conclusion**

In MVP patients, tenting volume index, an indicator of leaflet tethering, is strongly associated with MR severity, giving rise to an MVP with secondary leaflet tethering phenotype featuring more advanced morphological and hemodynamical characteristics. Whether secondary leaflet tethering in MVP impacts the result

of surgical repair or whether it could be a complementary therapeutic target should be further investigated in a larger patient group.

### Acknowledgements

The data supporting this study are available on request from the corresponding author. The protocol of this study was approved by the institutional review board of Zhongshan Hospital. Written informed consent was obtained at the time of consent for the clinical TEE procedure in all of the patients.

### Data Available Statement

Data Are available upon request from the authors.

**Funding Statement:** This work was supported in part by the Shanghai Municipal Health Commission (NO. 202140291), the Clinical Research Plan of Shanghai Hospital Development Center (Grant No. SHDC2020CR4071) and the Youth Fund Program in Zhongshan Hospital, Fudan University (Grant No.2021ZSQN16 & 2021-006ZP)

**Conflict of Interest: None**

### Reference

- [1] Adams D H, Rosenhek R, Falk V. Degenerative mitral valve regurgitation: best practice revolution [J]. *Eur Heart J*, 2010, 31(16): 1958-66.
- [2] Zoghbi W A, Adams D, Bonow R O, et al. Recommendations for Noninvasive Evaluation of Native Valvular Regurgitation A Report from the American Society of Echocardiography Developed in Collaboration with the Society for Cardiovascular Magnetic Resonance [J]. *J Am Soc Echocardiog*, 2017, 30(4): 303-71.
- [3] Grayburn P A, Berk M R, Spain M G, et al. Relation of echocardiographic morphology of the mitral apparatus to mitral regurgitation in mitral valve prolapse: Assessment by Doppler color flow imaging [J]. *Am Heart J*, 1990, 119(5): 1095-102.
- [4] Enriquez-Sarano M, Basmadjian A-J, Rossi A, et al. Progression of mitral regurgitation A prospective Doppler echocardiographic study [J]. *J Am Coll Cardiol*, 1999, 34(4): 1137-44.
- [5] Uretsky S, Supariwala A, Nidadovolu P, et al. Quantification of left ventricular remodeling in response to isolated aortic or mitral regurgitation [J]. *J Cardiovasc Magn Reson*, 2010, 12(1): 32.
- [6] Clavel M-A, Mantovani F, Malouf J, et al. Dynamic phenotypes of degenerative myxomatous mitral valve disease: quantitative 3-dimensional echocardiographic study [J]. *Circulation Cardiovasc Imaging*, 2015, 8(5): e002989.
- [7] Lee A P-W, Hsiung M C, Salgo I S, et al. Quantitative Analysis of Mitral Valve Morphology in Mitral Valve Prolapse With Real-Time 3-Dimensional Echocardiography [J]. *Circulation*, 2013, 127(7): 832-41.
- [8] Otani K, Takeuchi M, Kaku K, et al. Evidence of a Vicious Cycle in Mitral Regurgitation With Prolapse [J]. *Circulation*, 2012, 126(11\_suppl\_1): S214-S21.
- [9] Sakaguchi T, Kagiya N, Toki M, et al. Residual Mitral Regurgitation After Repair for Posterior Leaflet Prolapse-Importance of Preoperative Anterior Leaflet Tethering [J]. *J Am Heart Assoc*, 2018, 7(11).
- [10] Oguz D, Eleid M F, Dhesi S, et al. Quantitative Three-Dimensional Echocardiographic Correlates of Optimal Mitral Regurgitation Reduction during Transcatheter Mitral Valve Repair [J]. *J Am Soc Echocardiogr*, 2019, 32(11): 1426-35 e1.
- [11] Ge Z, Pan W, Li W, et al. Impact of Leaflet Tethering on Residual Regurgitation in Patients With Degenerative Mitral Disease After Interventional Edge-to-Edge Repair [J]. *Front Cardiovasc Med*, 2021, 8: 647701.

- [12] Saito K, Okura H, Watanabe N, et al. Influence of Chronic Tethering of the Mitral Valve on Mitral Leaflet Size and Coaptation in Functional Mitral Regurgitation [J]. *Jacc Cardiovasc Imaging*, 2012, 5(4): 337-45.
- [13] Kagiya N, Hayashida A, Toki M, et al. Insufficient Leaflet Remodeling in Patients With Atrial Fibrillation [J]. *Circulation Cardiovasc Imaging*, 2018, 10(3): e005451.
- [14] Ge Z, Pan W, Zhou D, et al. Effect of a novel transcatheter edge-to-edge repair device on the three-dimensional geometry of mitral valve in degenerative mitral regurgitation [J]. *Catheter Cardiovasc Interv*, 2021, 97(1): 177-85.
- [15] Malkowski M J, Boudoulas H, Wooley C F, et al. Spectrum of structural abnormalities in floppy mitral valve echocardiographic evaluation [J]. *Am Heart J*, 1996, 132(1): 145-51.
- [16] Delling F N, Kang L L, Yeon S B, et al. CMR Predictors of Mitral Regurgitation in Mitral Valve Prolapse [J]. *Jacc Cardiovasc Imaging*, 2010, 3(10): 1037-45.
- [17] El-Tallawi K C, Kitkungvan D, Xu J, et al. Resolving the Disproportionate Left Ventricular Enlargement in Mitral Valve Prolapse Due to Barlow Disease Insights From Cardiovascular Magnetic Resonance [J]. *Jacc Cardiovasc Imaging*, 2021, 14(3): 573-84.
- [18] Gaasch W H, Meyer T E. Left Ventricular Response to Mitral Regurgitation [J]. *Circulation*, 2008, 118(22): 2298-303.
- [19] Morningstar J E, Gensemer C, Moore R, et al. Mitral Valve Prolapse Induces Regionalized Myocardial Fibrosis [J]. *J Am Heart Assoc*, 2021, 10(24): e022332.
- [20] Kitkungvan D, Nabi F, Kim R J, et al. Myocardial Fibrosis in Patients With Degenerative Mitral Regurgitation With and Without Prolapse [J]. *J Am Coll Cardiol*, 2018, 72(8): 823-34.
- [21] Otsuji Y, Kumanohoso T, Yoshifuku S, et al. Isolated annular dilation does not usually cause important functional mitral regurgitation Comparison between patients with lone atrial fibrillation and those with idiopathic or ischemic cardiomyopathy [J]. *J Am Coll Cardiol*, 2002, 39(10): 1651-6.
- [22] Lee A P-W, Jin C-N, Fan Y, et al. Functional Implication of Mitral Annular Disjunction in Mitral Valve Prolapse A Quantitative Dynamic 3D Echocardiographic Study [J]. *Jacc Cardiovasc Imaging*, 2017, 10(12): 1424-33.
- [23] Tang Z, Fan Y-T, Wang Y, et al. Mitral Annular and Left Ventricular Dynamics in Atrial Functional Mitral Regurgitation: A Three-Dimensional and Speckle-Tracking Echocardiographic Study [J]. *J Am Soc Echocardiog*, 2019, 32(4): 503-13.
- [24] Ormiston J A, Shah P M, Tei C, et al. SIZE AND MOTION OF THE MITRAL-VALVE ANNULUS IN MAN .1. A TWO-DIMENSIONAL ECHOCARDIOGRAPHIC METHOD AND FINDINGS IN NORMAL SUBJECTS [J]. *Circulation*, 1981, 64(1): 113-20.
- [25] Komoda T, Hetzer R, Oellinger J, et al. Mitral Annular Flexibility [J]. *J Cardiac Surg*, 1997, 12(2): 102-9.
- [26] Detaint D, Messika-Zeitoun D, Avierinos J-F o, et al. B-Type Natriuretic Peptide in Organic Mitral Regurgitation [J]. *Circulation*, 2005, 111(18): 2391-7.
- [27] Pizarro R, Bazzino O O, Oberti P F, et al. Prospective Validation of the Prognostic Usefulness of Brain Natriuretic Peptide in Asymptomatic Patients With Chronic Severe Mitral Regurgitation [J]. *J Am Coll Cardiol*, 2009, 54(12): 1099-106.

Table 1 Determinants of Severity of Mitral Regurgitation (3D Vena Contracta Area)

Variables	Univariable	Univariable	Multivariable	Multivariable	Multivariable
Variables	β	P Value	β	P Value	Partial R <sup>2</sup>
Annular Area index	0.396	0.000	-0.142	0.314	-0.110
Prolapse Volume index	0.214	0.050	0.391	0.000	0.390
Tenting Volume index	0.464	0.000	0.585	0.000	0.562
PVi + TVi	0.243	0.026	0.163	0.074	-0.190
AHCWR	-0.262	0.017	-0.167	0.067	-0.184

Univariate and multivariate linear regression analyses were performed.

Table 2 Clinical and two-Dimensional Echocardiographic Characteristics

	Control (N=20)	MVPt- (N=63)	MVPt+ (N=31)	P-Value
Age, years	66.5 (8.7)	74.1 (6.6)	73.7 (6.0)	<0.001*
Men, n (%)	11(55)	25 (40)	13 (42)	
BSA, m <sup>2</sup>	1.7 (0.2)	1.5 (0.2)	1.6 (0.2)	<0.001*
NYHA, n (%)				<0.001*
1	23 (100.0)	0(0)	0(0)	
2	0(0)	15 (23.8)	4 (12.9)	
3	0(0)	39 (61.9)	20 (64.5)	
4	0(0)	9 (14.3)	7 (22.6)	
NT-proBNP	-	885.2±1298.76	1870.35±2266.97	<0.001
VCA, cm <sup>2</sup>	0.0 (0.0)	0.6 (0.2)	0.9 (0.3)	<0.001*¶
LVEDVi, mL/m <sup>2</sup>	46.1 (10.6)	72.3 (15.8)	86.4 (22.0)	<0.001*¶
LVESVi, mL/m <sup>2</sup>	17.5 (4.7)	28.2 (10.1)	35.0 (14.1)	<0.001*¶
LVEF, %	63.2 (3.3)	60.4 (11.8)	56.4 (17.3)	0.13
VCW, mm	0.0 (0.0)	8.9 (2.7)	8.8 (1.5)	<0.001*
Etiology, n (%)				0.274
FED	-	55 (87)	30 (97)	
Barlow	-	8 (13)	1 (3)	
Flail, n (%)	0(0)	46 (73.0)	29 (93.5)	<0.001*¶
Flail width, mm	0.0 (0.0)	11.8 (3.3)	12.5 (2.9)	<0.001*
Flail gap, mm	0.0 (0.0)	7.3 (2.9)	9.2 (2.2)	<0.001*¶
AML length, mm	21.6 (3.4)	24.5 (3.9)	25.6 (3.9)	0.001*
PML length, mm	11.9 (1.6)	16.5 (3.4)	18.1 (3.0)	<0.001*¶
AP diameter(2D), mm	30.3 (6.7)	33.3 (4.9)	36.0 (3.2)	<0.001¶
LVEDD, mm	46.2 (2.9)	52.1 (4.8)	55.1 (5.2)	<0.001*¶
LVESD, mm	29.3 (3.4)	31.7 (3.3)	35.4 (6.6)	<0.001*¶
LAA, cm <sup>2</sup>	18.0 (5.0)	29.1 (8.3)	33.0 (9.5)	<0.001*
sPAP, mmHg	-	51.8±18.9	60.8±17.5	0.052

AML, anterior mitral leaflet; PML, posterior mitral leaflet; FED, fibroelastic deficiency; BD, barlow disease; LVEDVi, left ventricular end-diastolic volume index; LVESVi, left ventricular end-systolic volume index; LVEF, left ventricular ejection fraction; VCW, vena contracta width; sPAP, systolic pulmonary artery pressure; LAA, left atrial area. \* P < 0.05 for MVPt- versus control, | P < 0.05 for MVPt+ versus control, ¶ P

< 0.05 for MVPt+ versus MVPt-.

Table 3 3D Geometry of Mitral Complex in healthy controls, MVPt- and MVPt+ patients

	Control (n=20)	MVPt- (n=63)	MVPt+ (n=31)	ANOVA
ALPMi, mm/m <sup>2</sup>	20.2 (2.1)	23.0 (3.0)	24.5 (3.1)	<0.001* <sup>¶</sup>
APi, mm/m <sup>2</sup>	18.5 (2.1)	21.2 (2.6)	23.1 (2.7)	<0.001* <sup>¶</sup>
Annular Height, mm	5.6 (1.4)	6.3 (1.7)	6.6 (1.6)	0.142
AAi, mm <sup>2</sup> /m <sup>2</sup>	494.6 (79)	616.5 (109.6)	734.7 (128.1)	<0.001* <sup>¶</sup>
AML Angle, *	19.1 (6.7)	16.7 (6.5)	24.8 (5.0)	<0.001 <sup>¶</sup>
PML Angle, *	25.0 (6.3)	23.9 (7.4)	31.0 (5.6)	<0.001 <sup>¶</sup>
THi, mm <sup>2</sup> /m <sup>2</sup>	2.3 (0.7)	2.6 (1.1)	4.8 (1.4)	<0.001* <sup>¶</sup>
PHi, mm <sup>2</sup> /m <sup>2</sup>	0.8 (0.5)	3.6 (1.7)	2.9 (1.5)	<0.001*
TVi, mL/m <sup>2</sup>	0.4 (0.2)	0.4 (0.2)	1.2 (0.4)	<0.001 <sup>¶</sup>
PVi, mL/m <sup>2</sup>	0.1 (0.1)	0.4 (0.3)	0.3 (0.3)	<0.001*
ACi, mm <sup>2</sup> /m <sup>2</sup>	61.0 (6.1)	73.0 (8.3)	78.7 (9.4)	<0.001* <sup>¶</sup>
Ellipticity, (%)	115.2 (11.3)	109.1 (10.7)	106.4 (8.4)	0.008*
TVi + PVi, mL/m <sup>2</sup>	0.4 (0.1)	0.9 (0.5)	1.1 (0.5)	<0.001*
AHCWR (%)	16.2 (4.3)	18.2(5.3)	17.3(4.0)	0.117

ALPM, anterior-lateral/posterior-medial diameter index; AP, anterior-posterior diameter index; THi, tenting height index; PHi, prolapse volume index; TVi, tenting volume index; PVi, prolapse volume index; ACi, annular circumference index; AML, anterior mitral leaflet; PML, posterior mitral leaflet

**Figure 1** 3D parametric models (D) of patient’s mitral valve by MVN analysis. Three orthogonal mitral annulus images, including two-chamber view (A), long-axis view (B) and short-axis view (C) were displayed and subsequently used to model the entire annulus and mitral valve.

**Figure 2** A: Scatterplots demonstrating the distribution of tenting volume index among healthy controls and MVP patients and the cutoff value of 0.7 mL/m<sup>2</sup> (horizontal dashed line) to distinguish the occurrence of secondary leaflet tethering in MVP patients. B to E: Histograms comparing the tenting volume index (B), annular area index, prolapse volume index and AHCWR between the healthy controls, MVPt- and MVP+ group.

**Figure 3** Correlations of tenting volume index with NT-proBNP and 3D VCA. The scatterplot demonstrates a mild correlation between tenting volume index and NT-proBNP (A) and 3D VCA (B). C: ROC curve for 3D VCA to predict the occurrence of secondary leaflet tethering.

**Figure 4** Illustrative examples of mitral valve prolapse patients without and with secondary leaflet tethering. A mitral valve prolapse patients without secondary leaflet tethering (PVi = 0.69 mL/m<sup>2</sup>, tenting volume index = 0.19 mL/m<sup>2</sup>, VCA = 0.32 cm<sup>2</sup>) B and C mitral valve prolapse patients with secondary leaflet tethering and larger regurgitant orifices. Case B PVi = 0.02 mL/m<sup>2</sup>, tenting volume index = 1.46 mL/m<sup>2</sup>, VCA = 0.95 cm<sup>2</sup>; Case C PVi = 0.25 mL/m<sup>2</sup>, tenting volume index = 2.2 mL/m<sup>2</sup>, VCA = 1.48 cm<sup>2</sup>)

**Figure 1**

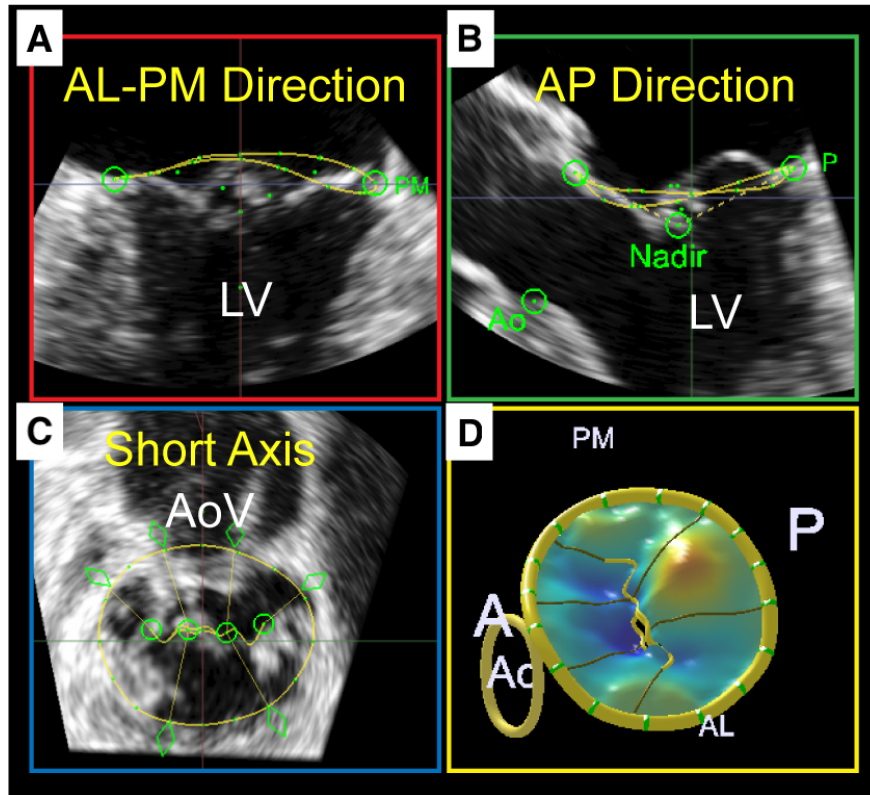


## Figure 2

### Hosted file

image2.emf available at <https://authorea.com/users/612415/articles/640321-secondary-leaflet-tethering-in-patients-with-degenerative-mitral-regurgitation-and-its-association-with-the-severity-of-mitral-regurgitation>

## Figure 3

### Hosted file

image3.emf available at <https://authorea.com/users/612415/articles/640321-secondary-leaflet-tethering-in-patients-with-degenerative-mitral-regurgitation-and-its-association-with-the-severity-of-mitral-regurgitation>

## Figure 4

